Applied Thermal Engineering 225 (2023) 120162

Contents lists available at ScienceDirect

Applied Thermal Engineering

journal homepage: www.elsevier.com/locate/apthermeng

Research Paper

Enhanced behaviour of a passive thermoelectric generator with phase change heat exchangers and radiative cooling

David Astrain [a,*], Juliana Jaramillo-Fernandez [b], Miguel Araiz [a], Achille Francone [b], Leyre Catalán [a], Alejandra Jacobo-Martín [b], Patricia Alegría [a], Clivia M. Sotomayor-Torres [b,c]

[a] Engineering Department, Smart Cities Institute, Public University of Navarre, Campus Arrosadía s/n, 31006 Pamplona, Spain
[b] Catalan Institute of Nanoscience and Nanotechnology (ICN2), CSIC and BIST, Campus Universitat Autonoma de Barcelona (UAB), Bellaterra, Barcelona 08193, Spain
[c] ICREA—Institució Catalana de Recerca i Estudis Avançats, Barcelona 08010, Spain

ARTICLE INFO

Keywords:
Radiative cooling
Heat-pipe
Thermoelectric generator
Thermal resistance

ABSTRACT

Heat exchangers are essential to optimize the efficiency of Thermoelectric Generators (TEGs), and heat pipes without fans have proven to be an advantageous design as it maintains the characteristic robustness of thermoelectricity, low maintenance and lack of moving parts. However, the efficiency of these heat exchangers decreases under natural convection conditions, reducing their heat transfer capacity and thus thermoelectric power production. This work reports on a novel heat exchanger that combines for the first time, phase change and radiative cooling in a thermoelectric generator to improve its efficiency and increase the production of electrical energy, specially under natural convection. For this, two thermoelectric generators with heat-pipes on their cold sides have been tested: one with the radiative coating and the other without it. Their thermal resistances have been determined and the electric power output was compared under different working conditions, namely, natural convection and forced convection indoors and outdoors. The experimental tests show a clear reduction of the heat exchanger thermal resistance thanks to the radiative coating and consequently, an increase of electric production 8.3 % with outdoor wind velocities of 1 m/s, and up to 54.8 % under free convection conditions. The application of the radiative surface treatment is shown to result in a more stable electrical energy production, suppressing the drastic decrease in the generated electric power that occurs in thermoelectric generators when they work under free convection.

1. Introduction

Thermoelectric generators (TEG) are devices capable of converting thermal energy into electricity without moving parts, which leads to important advantages such as robustness and reliability, lower price, absence of noise and vibrations, and scalability [1,2]. These characteristics, together with the need to increase power generation with renewable sources, has led to an important research activity in these fields, developing, as a consequence, interesting and innovative applications for TEGs using different thermal sources for the production of electricity [3]. Thus, for example, Montecuco et al. [4] developed a thermoelectric stove capable of generating 600 W of domestic hot water, producing at the same time 27 W of electrical power, by means of a combustion TEG equipped with a water pumping system. Zheng et al. [5] developed a prototype of a domestic thermoelectric co-generator, harnessing the waste heat present in the exhaust pipe to produce hot water and electricity. Mohammadnia et al. [6] investigated the combination of thermoelectricity in solar concentration systems with a Stirling engine, and Karri et al. [7] achieved savings of up to 3 % in the fuel consumption of a SUV-type vehicle, thanks to the TEG placed in the exhaust pipes.

However, the main drawback of TEGs is their low efficiency in energy conversion, obtaining values close to 3 % for a temperature difference of 120 °C, while for the same temperature difference, systems based on Organic Rankine Cycles achieve an efficiency of 10 % [8]. This is why there are important efforts in the improvement of the thermoelectric materials [9], but also in the optimization of the heat exchangers, at both the hot and cold sides of the device. As demonstrated by Astrain et al. [10], a 10 % decrease in the thermal resistance of the heat exchangers causes an 8 % increase in the generation of electric energy from a TEG. As a consequence, water heat exchange systems are used in many applications of TEGs, such as in Niu et al. [11] which analyzed the power generation of a TEG using water heat exchangers

* Corresponding author.
E-mail addresses: david.astrain@unavarra.es (D. Astrain), juliana.jaramillo@icn2.cat (J. Jaramillo-Fernandez).

https://doi.org/10.1016/j.applthermaleng.2023.120162
Received 8 September 2022; Received in revised form 16 January 2023; Accepted 31 January 2023
Available online 3 February 2023

Nomenclature

E_t	Electromotive force, V
b_x	Uncertainty of parameter x
I	Electric current, A
K	Thermal conductance, W/K
$\dot{Q}_C$	Heat released from the cold side, W
$\dot{Q}_H$	Heat absorbed in the hot side, W
R_0	Electric resistance of the TE modules, Ω
R_C	Cold side thermal resistance, K/W
R_H	Hot side thermal resistance, K/W
R_L	Load resistance, Ω
T_C	Cold side temperature of the modules, °C
T_H	Hot side temperature of the modules, °C
T_{source}	Heat source temperature, °C
T_∞	Environment temperature, °C
V	Output voltage, V
$\dot{W}_e$	Electric power output, W

Greek symbols

α	Seebeck's coefficient, V/K
$\in$	Efficiency

Abbreviations

IPA	Isopropyl alcohol
IR	Infrared
HP	Heat-pipe
NIL	Nanoimprint Lithography
PDMS	Poly dimethyl siloxane
TEG	Thermoelectric generator
TEG_RC	Thermoelectric generator with radiative treatment on the heat-pipes
TEG_w/o_RC	Thermoelectric generator without any treatment on the heat-pipes
TEM	Thermoelectric module
UV	Ultraviolet
VIS	Visible

where the pressure losses, different water flows and temperature sources were taken into account. The prototype developed by Kim et al. [12], which achieved a maximum power output of 119 W with 40 thermoelectric modules, cooled with a channel heat exchanger through which water circulated at an inlet temperature of 20 °C. However, these systems require a pump that moves the liquid through the device, in addition to dissipating the heat absorbed by the fluid to the environment through another heat exchanger, usually with a fan. Aranguren et al. [13] took these factors into account, studying the influence of the mass flow rate of the water in the channel heat exchanger, the air flow in the water-to-ambient heat sink, as well as the pressure losses in the system. Their most important conclusion was that in many cases, the electrical consumption of the pump and the fan necessary to dissipate the heat, did not compensate for the increase in the power output of the TEG by the reduction in thermal resistances.

A significant advance to improve the efficiency of the heat exchangers in thermoelectric applications is the use of heat pipes (HP), where, thanks to the phase change, the entire convective area in contact with the air is used, as it is able to distribute the heat flow, from the thermoelectric modules throughout the area. Yan Liu et al. [14] developed a TEG prototype with HP as heatsinks, working with air and water. Thanks to the low thermal resistances of the heat exchangers, they obtained up to 6 W of electric power per thermoelectric assembly. Aranguren et al. [15] showed that a TEG that uses HP with fans, to harvest waste heat from a chimney, produces 43 % more electric power than a TEG using finned heat sinks under the same working conditions.

All these heat exchange systems mentioned obtain thermal resistance values very suitable for thermoelectric applications. However, they have the disadvantage of using devices with moving parts, such as fans or pumps, which, in addition to complicating the installation, consume electricity. In all these applications, the intrinsic advantages of thermoelectricity of being a technology without moving parts is lost. In order to study applications of TEGs free of moving parts, and recover this advantage of thermoelectricity, heat exchangers without fans or pumps to drive the fluids have been developed. Thus, for example, Date et al. [16] compared the use of finned heatsinks of different geometries with passive HPs as the heat exchanger of the cold side of a TEG. The electric power output produced with the HP-TEG system was 1.8 W, which is 4 times higher than the electric generation of the TEG that used the finned device. Orr et al. [17] employed a fan-less HP in their experimental work with TEGs, obtaining 6 W per thermoelectric module and an efficiency in the conversion of 2.3 %. Araiz et al. [18] developed a TEG that generates 259 W/m^2 of net power from waste heat in an industry, employing biphasic thermosyphon heat exchangers, capable of working under natural convection conditions.

This type of TEGs without moving parts are widely used in remote sensor applications, such as the one reported in the work of Huang et al. [19], who developed a thermoelectric micro generator to power surveillance sensors in forests. Catalan et al. [20,21] developed a TEG using HPs without fans, capable of feeding a remote volcanic monitoring station installed on Teide's volcano. In this work, the importance of the lack of moving parts was highlighted since it provides the necessary robustness for this application. However, the authors also reported how the electric generation of this application decreased by 25 % when the wind speed dropped to values below 1 m/s. Similarly, Alegría et al. [22] built a TEG prototype to harvest geothermal energy, with fan-less heat-pipes. Their results showed the loss of efficiency when there is no wind, due to the increase in the thermal resistance of the HPs, going from 35 W of power output with 1.5 m/s of wind, to 20 W of electric generation without wind, equivalent to a reduction of 33 %.

In order to solve these cited problems of TEGs and to increase their efficiency, maintaining the ability of working without moving parts, this work presents, for the first time, the combination of heat pipes with radiative cooling, applied to the TEGs.

The goal is to improve the thermal resistance values of heat pipes heat exchangers that work without fans, especially when the wind velocity is very low or zero. In these circumstances, the heat transfer from the outer surface of the HP to the air happens under natural convection, with very low convection heat transfer coefficient values (between 3 and 10 W/m^{2}K), so that thermal radiation mechanisms, which are always present, become more important [23]. The focus of this study is on enhancing the overall heat transfer from the heat pipes to the air, under natural convection, by improving the HP's radiative properties at thermal wavelengths (from 2.5 up to 25 μm). This is achieved by coating the copper envelope surface of the HPs with a thin broadband thermal emitter that consist of a micro-structured resist. It enables strong emittance in the mid-infrared (mid-IR), and high transparency in the visible (VIS) and near-infrared (near-IR). This preserves the high reflectance of cooper in the visible spectral range, while maximizing the cooling capability of naturally cooled HPs, by changing the radiative properties of the copper envelope surface in the mid-IR, from highly reflective to highly emitting (See Supplementary Information). In this manner, the overall heat transfer of the naturally cooled HPs is enhanced via radiation, which has a critical role under these conditions. Furthermore, the advantages of TEGs that operate without moving parts are maintained, as discussed above. This work is based on the emerging technique of

radiative cooling, which enables the cooling of objects that are facing the sky even during daytime, without consuming energy. This passive process generally consists on maximising the radiated power while minimizing the heat gain due to solar and atmospheric absorption. This can be achieved by engineering the optical properties of materials, i) minimizing the absorption of sunlight and atmospheric thermal radiation and (ii) enhancing their emittance in the mid-IR, as the energy radiated is directly proportional to the surface emissivity. This broadband mid-IR emittance is particularly relevant for above-ambient cooling applications, e.g. when the substrate emits a large amount of heat, such as in a thermoelectric generator, because it maximizes the power evacuated as thermal radiation. Furthermore, for outdoor applications, a net heat exchange between the surface and the outer space takes place due to the surface high emittance from 8 to 13 μm, the spectral range at which the atmosphere is transparent. As the blackbody thermal radiation peaks at ~ 10 μm at 300 K, the highly emitting surface is able to dissipate heat through the infrared transparency window (8–13 μm).

Many radiative cooling materials have by now been demonstrated, using nanotechnology and surface engineering. Remarkable approaches include thin film multi-layer structures [24–28], microsphere-based photonic media [29–31] metal-dielectric nanophotonic structures [32], double-layer nanoparticle-based coatings [33,34], aerogels [35,36], hybrid dielectric-polymer materials [37–40], porous synthetic polymer based coatings [35,38,41,42] and sustainable cellulose-based films [43–49].

However, the application of radiative cooling materials for thermoelectric generators has been barely studied, despite its potential impact to enhance electric generation. For example, Zhan et al. [50] applied this radiative enhancement technique to thermoelectricity. In their work, this surface treatment was applied to a finned heatsink in natural convection, increasing the electric generation from 0.018 W to 0.028 W, using a heat source at a temperature of 250 °C. Their work showed that the improvement achieved in finned dissipaters thanks to a radiative treatment, results in an increased thermoelectric generation of more than 50 % under these conditions. Since finned heat sinks were used as heat exchangers, the generation obtained is rather low, around 28 mW. However, it showed that advances in this technology could lead to more efficient heat exchangers.

In summary, there are many published papers that study phase change heat exchanger in thermoelectric generators and a few very recent works about radiative cooling and thermoelectric generators. However, radiative cooling and phase change heat exchangers combined in a thermoelectric generator have not been reported so far. In this work a passive thermoelectric generator, which includes phase change heat exchangers and radiative cooling has been developed and tested for the first time. Thanks to this novel heat exchanger, the passive thermoelectric generator produces 58 % more electrical energy under natural convection. This approach could be used to improve applications of thermoelectric generation that do not incorporate moving parts, thus preserving the intrinsic advantages of thermoelectricity such as robustness, reliability and lack of noise and vibrations.

2. Methodology

2.1. Thermoelectric generators and heat exchangers

Thermoelectric generators are devices capable of converting heat into electric energy. Their principle of operation is based on the heat transfer from the hot source to the hot side of the thermoelectric modules (TEM), where part of that heat flow will be transformed into electric energy, thanks to the Seebeck effect. The rest of the heat will be released to the environment by another heat exchanger placed at the cold side of the modules, as shown in Fig. 1.

According to the basic calculation method [51], the rate of heat flow that reaches the hot face of the thermoelectric modules is given by Eq. (1) and contemplates the Peltier effect, the Joule effect and the Fourier's law of heat conduction. With the same effects, but making the energy balance on the cold side, the rate of heat flow that the thermoelectric module releases to the environment through the heat exchanger is given by Eq. (2). Likewise, and due to the Seebeck effect, an electromotive force is produced in the thermoelectric module whose expression is given by Eq. (3). The values for the thermal conductance, electric resistance, Seebeck coefficient and temperature operation range vary with the TEM used. In this work Marlow TG12-8L [52] thermoelectric modules have been employed.

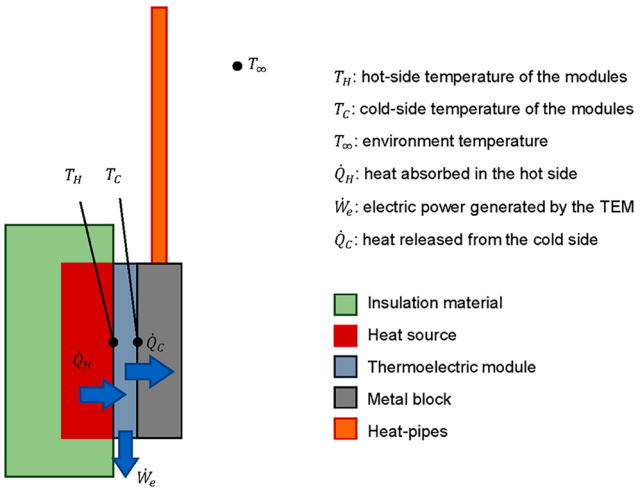

Fig. 1. Thermoelectric Generator scheme and temperatures at different locations of the TEG with integrated heat pipes.

$$\dot{Q}_H = K(T_H - T_C) - \frac{I^2 R_0}{2} + \alpha I T_H \tag{1}$$

$$\dot{Q}_C = K(T_H - T_C) + \frac{I^2 R_0}{2} + \alpha I T_C \tag{2}$$

$$E_t = \alpha(T_H - T_C) \tag{3}$$

If the thermoelectric generator is connected to a load resistance, R_L, there will be an output voltage in the load resistance given by Eq. (4).

$$V = E_t - R_0 I = R_L I \tag{4}$$

So, the electric power produced by the generator will be determined by Eq. (5), where $m = R_L/R_0$; and its efficiency is given by Eq. (6).

$$\dot{W}_e = \alpha(T_H - T_C)^2 \frac{m}{R_0(m+1)^2} \tag{5}$$

$$\epsilon = \frac{\dot{W}_e}{\dot{Q}_H} = \frac{T_H - T_C}{T_H} \frac{m}{1 + m - \frac{(T_H - T_C)}{2T_H} + (1+m)^2 \frac{R_0 k}{\alpha^2 T_H}} \tag{6}$$

The temperatures of the hot, T_H, and cold, T_C, sides of the thermoelectric modules will depend on the temperatures of the hot source and cold sink (environment), as well as on the heat transfer rate and the thermal resistances of the heat exchangers used, whose expressions are given by Eq. (7) and Eq. (8).

$$R_H = \frac{T_{source} - T_H}{\dot{Q}_H} \tag{7}$$

$$R_C = \frac{T_C - T_\infty}{\dot{Q}_C} \tag{8}$$

As can be deduced from these equations, a decrease in the thermal resistance of the heat exchangers will mean a greater temperature difference between the faces of the thermoelectric modules, increasing the generation of electric power and the efficiency of the system, see Eq. (5) and (6). This effect was already demonstrated by Astrain et al. [10],

showing that the efficiency of the TEG was improved by 8 % when the thermal resistance of the heat exchangers was decreased by 10 %.

This experimental study is only focused on the cold side of the thermoelectric modules and using heat pipes as heat exchangers on the cold side since, as shown in [15,16], these heat exchangers improve the electric generation of the TEGs, with respect to those that use finned heat sinks.

Two identical TEG prototypes have been built, so that each of them consists of a heating plate responsible for supplying a heat flux to the thermoelectric generator. Over this plate a thermoelectric module, model Marlow TG12-8L [52], with 127 BiTe pairs, has been placed. On the cold side of the module, a 40 mm × 40 mm × 12 mm aluminum plate has been located, where 3 heat pipes, whose length is 400 mm and have 8 mm diameter, have been inserted to transfer the heat to the environment, as shown in Fig. 2. All these components have been assembled with two steel metal plates and screws, making a tightening of 1 Nm. Finally, with the aim that all the heat generated by the heating plate is transferred to the thermoelectric modules, all this assembly has been properly insulated, except for the HP, which are responsible for releasing the heat to the environment. For this, a first layer of 60 mm rockwool material Pro Rox WM 970 ES [53] has been placed, with a thermal conductivity of 0.04 W/mK within the range of the working temperatures. Over this material a second 20-mm layer of ARMAFLEX has been placed [54].

2.2. Experimental methodology

One of the objectives of this work is to determine the influence of the application of the radiative treatment, described in Section 2.3, on the performance of heat-pipe based heat exchangers for the cold side of thermoelectric generators under different working conditions (forced and natural convection, indoor and outdoor conditions). To do this, it is necessary to determine the thermal resistance of the HP, as well as the electric power output obtained with the TEGs. Consequently, two prototypes have been built: TEG_RC, a thermoelectric generator using a HP that includes a radiative cooling treatment, TEG_w/o_RC, another thermoelectric generator using a heat-pipe too, but without any radiative treatment. Both prototypes include NiCr-Ni thermocouples temperature probes on the hot and cold sides of the thermoelectric modules. The environment temperature is also measured using an additional temperature probe, as shown in Fig. 1. Likewise, the heat flux provided by the electric resistances acting as the heat source has been measured by an ammeter and voltmeter. Each thermoelectric generator is connected to a variable load resistance and has an ammeter and voltmeter to be able to register the power output coming from them. All these variables have been recorded during the experimentation with an Ahlborn Almemo 5690-1M09 data acquisition system. Table 1 includes the resolution and accuracy for every measurement probe that has been employed in the tests.

From these experimental results, the two variables under study can be estimated: the thermal resistance of the HP heat exchangers on the cold side of the thermoelectric modules can be found using Eq. (8), where $\dot{Q}_C$, which is the rate of heat flow released to the environment, can be estimated following the energy balance in Eq. (9).

$$\dot{Q}_H = \dot{W}_e + \dot{Q}_C \tag{9}$$

Here, $\dot{Q}_H$, can be obtained from Eq. (10), assuming that the device is properly insulated, and the thermal losses can be neglected; and $\dot{W}_e$ is the electric power output from the thermoelectric module, see Eq. (11). A temperature sensor was placed outside the insulation box covering the heating plate. Since the temperature measurements were close to the environmental temperature sensor, the thermal losses throughout this material can be neglected.

$$\dot{Q}_H = V_{re} I_{re} \tag{10}$$

$$\dot{W}_e = V_p I_p \tag{11}$$

The performance of the thermoelectric generators was studied under several conditions. They were connected to different load resistances to obtain the characteristic curve of the generator. The goal was to prove the influence of the radiative surface treatment (described in Section

Table 1
Resolution and accuracy of the measurement sensors.

Sensor	Resolution	Accuracy
Temperature (°C)	0.1	± 0.5
Ammeter (A)	0.01	± 0.02
Voltmeter (V)	0.1	± 0.4

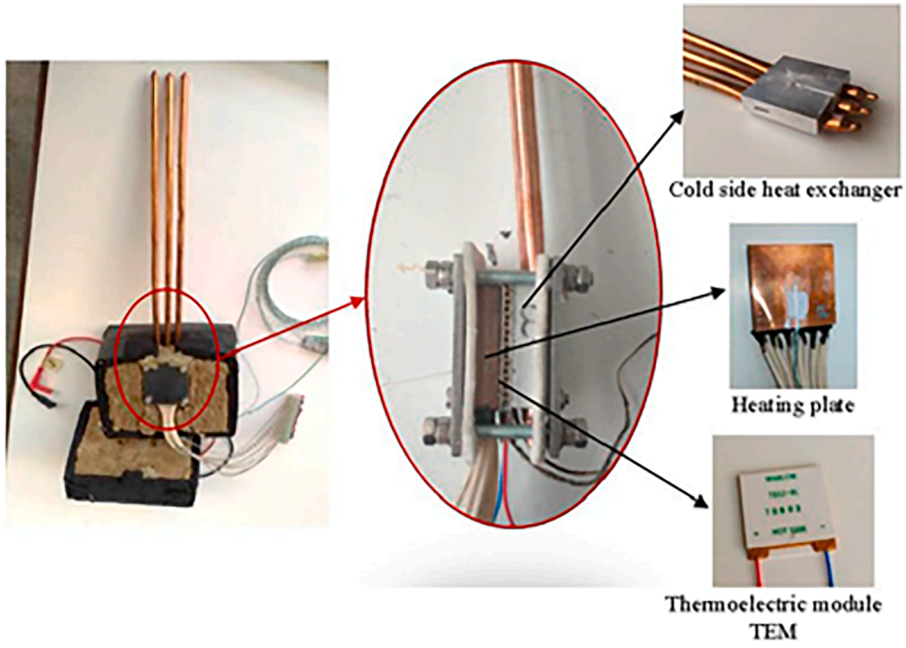

Fig. 2. Thermoelectric Generator prototype with a heat-pipe on the cold side.

2.3) not only on the performance of the heat exchangers, but also on the electric generation of the prototypes under different ambient conditions. The results obtained from a thermoelectric generator whose HPs have been coated with the radiative treatment (TEG_RC) were compared with the generator without the radiative cooling treatment (TEG_w/o_RC).

In the first test, both prototypes with no treatment were tested to know the initial conditions of each of them (TEST_0), with the aim of determining the uncertainty that could exist in the operation of both identical generators, due to possible differences in the manufacture and assembly processes. Once it was verified that they offer equivalent results, as shown in Fig. 4, one of them (TEG_RC) was treated with the radiative coating, as described in Section 2.3. Again, both generators were tested simultaneously inside a climatic chamber to maintain constant the environment temperature under conditions of forced convection with air speed of 1 m/s (TEST_1) and natural convection (TEST_2). Finally, tests (TEST_3) were carried out outdoors under real environment conditions. Table 2 summarises the tests performed in this work.

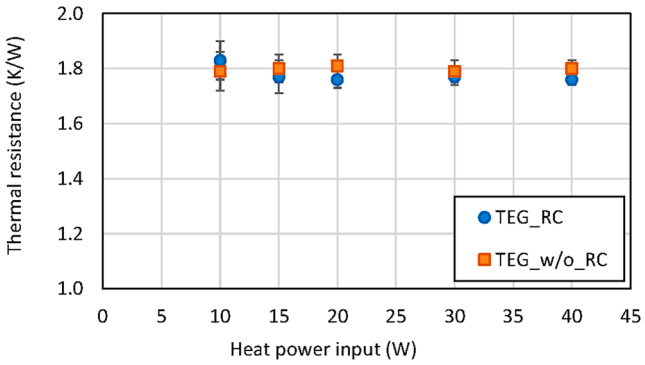

Fig. 4. TEST-0 for both prototypes TEG_RC and TEG_w/o_RC without any surface radiative treatment, at an air velocity of 1 m/s.

Table 2
Conditions of the tests carried out in this work.

TEST-0	TEST-1	TEST-2	TEST-3
Indoor Initial conditions	Indoor Forced convection	Indoor Natural convection	Outdoor Free - forced
TEG_RC: No treat. TEG_w/o_RC: No treat.	TEG_RC: With treat. TEG_w/o_RC: No treat.	TEG_RC: With treat. TEG_w/o_RC: No treat.	TEG_RC: With treat. TEG_w/o_RC: No treat.

2.3. Micro-patterning of the HPs integrated in the TEG system

The passive radiative cooling coating was applied on the external surface of the copper HPs integrated in the TEG system by means of UV assisted Nanoimprint Lithography (UV-NIL). The radiative cooling coating consists of a commercial resist with inherent high emissivity in the mid-IR. Its surface is texturized by using this nano- and micro-replication technology to further enhance its directional spectral emissivity, even at high emission angles.

In UV-NIL, the pattern is replicated from a mold into a low molecular weight photo-curable resist layer which is previously applied on the desired surface. Then, the polymer is crosslinked under UV light irradiation to produce a hard structured coating. Due to the HPs curved surface, the mold used in this case for the UV-NIL process was a thin soft flexible mold fabricated in poly dimethyl siloxane (PDMS) [55,56] which allows conformal contact with the whole curved surface. This working mold was fabricated using soft-lithography [57] by casting and curing the polymer precursors in direct contact with a 10 cm diameter silicon master mold, containing the topography to be replicated (fabricated with photolithography and electroplating techniques) [58]. Fig. 3**a** shows the soft-lithography procedure. A PDMS (Sylgard 184, Dow Corning, Sigma Aldrich) precursor in dilution with the curing agent

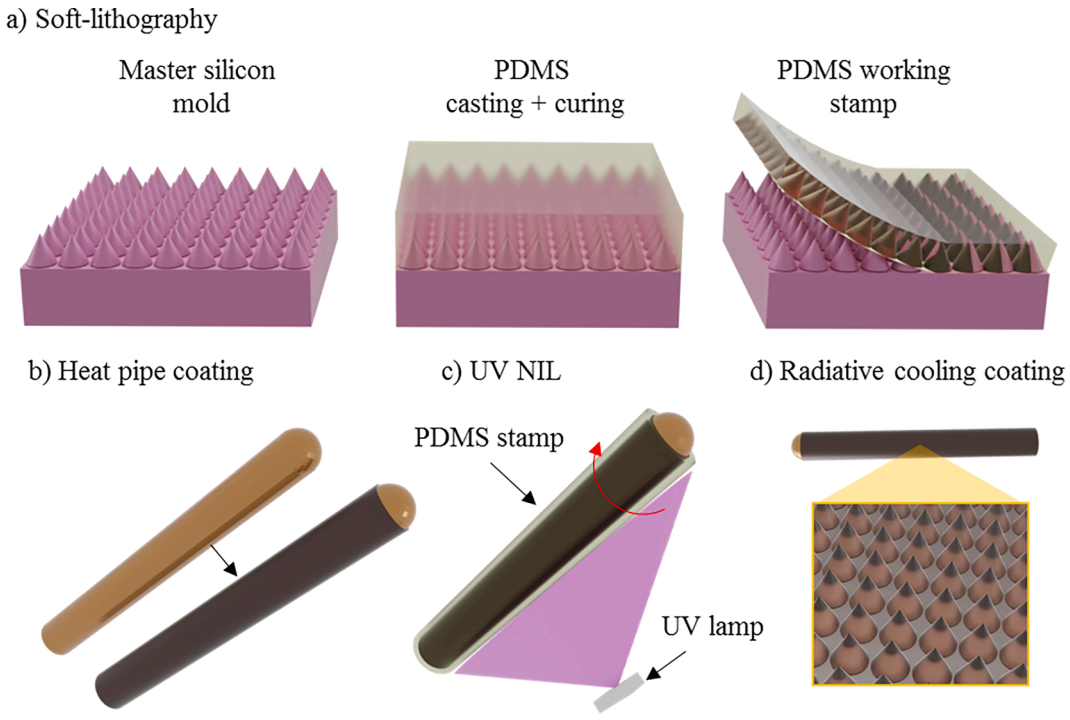

Fig. 3. Micro-patterning of the HPs integrated in a TEG system: a) PDMS working mold fabrication by soft-lithography technique. The PDMS precursor mixture is poured over the master silicon mold and after polymer crosslinking, the flexible PDMS is peeled off. b) After cleaning, the HP surface is coated by using a syringe, c) the PDMS working mold is wrapped around the coated HP surface, and irradiated by UV light to perform the UV-NIL process. d) Once the resist is crosslinked and the mold peeled off, the coated surface exhibits the required hardened topography.

(10:1) was mixed and degassed under vacuum. First, the PDMS solution was casted on top of the silicon master mold and then cured for 4 h at 80ºC. After polymer crosslinking, the PDMS mold was peeled-off manually and a flexible working mold, with about 2 mm thickness, was obtained.

The surface treatment began by cleaning the copper HPs with IPA and subsequently drying them properly. The commercial resist (3 ml) was applied on the copper HP surface (placed in a planar position) using a syringe (Fig. 3**b**). The PDMS flexible working mold was put into contact with the coated copper surface, wrapped around the pipe and finally tightened with metallic clips. In this way, a constant pressure was guaranteed along the whole contact area and the uncured resist was able to flow through the mold cavities. Afterwards, the wrapped HP was placed inside a homemade UV-NIL tool, whose chamber was previously fully covered with aluminium paper (to promote homogeneous UV illumination and facilitate the curing of the resist all around the curved surface of the HP during the exposure step). Then, the surface was irradiated by the UV lamp (OmniCure S2000-XLA), as shown in Fig. 3**c** (exposure time ~ 15 s). Finally, the mold was manually peeled off leaving the cured resist with the negative shape of the mold pattern on the surface of the copper bars, required to improve the material radiative properties (Fig. 3**d**).

3. Results and discussion

3.1. Uncertainty analysis and TEST-0

In the tests, the performance of each heat-pipe heat exchanger and thermoelectric generator has been analysed varying the heat flux absorbed from the hot side. When studying the thermal resistance of the heat exchangers, the tests were replicated three times to estimate the overall uncertainty according to Coleman [59], which is composed of the random standard uncertainty (using the replicas done) and the systematic uncertainty, using for every parameter the energy balances in Eq. (9), (10), (11) and the following Eq. (12).

$$b_{R_C}^2 = \left(\frac{1}{\dot{Q}_C}\right)^2 b_{T_C}^2 + \left(\frac{-1}{\dot{Q}_C}\right)^2 b_{T_\infty}^2 + \frac{(T_C - T_\infty)^2}{\dot{Q}_C^4} b_{\dot{Q}_C}^2 \quad (12)$$

Fig. 4 shows the results of the preliminary tests (TEST-0), that provides a comparison of the starting point of the heat exchangers and the initial operation of the two thermoelectric generators (TEG_RC and TEG_w/o_RC). In this way, it is possible to evaluate if the original prototypes exhibit differences in the thermal behavior, before applying any treatment. The objective is to eliminate the uncertainty in the results of the subsequent tests due to possible variations in the manufacture and assembly process of the prototypes. These tests have been carried out inside a climatic chamber with an air velocity of 1 m/s and an ambient temperature of 15 °C, for different heat fluxes supplied. As it can be seen from the results, both prototypes offer very similar thermal resistance, with maximum deviations of 0.05 K/W, which is below the calculated overall uncertainty, which for these tests is 0.07 K/W. In this way, it is ensured that, once the radiative surface treatment has been applied to one of the prototypes, the differences in their thermal and electrical behavior will be exclusively due to the applied coating and the resulting thermal improvement.

3.2. Results of indoor experiments: TEST-1 and TEST-2

Once it has been verified that there are no appreciable differences between the two prototypes, the HPs of one of them (TEG_RC) have been coated with the radiative surface treatment described in Section 2.3 and the thermal characterization tests have been repeated in both natural convection and forced convection with an air velocity of 1 m/s.

As mentioned in the methodology section, in each test, both TEG prototypes have been connected to an electrical load resistance and a heat flow is applied to them, recording the temperatures, the voltage and current in the thermoelectric modules as a function of time, until steady state is reached. Fig. 5 difference between the cold face of the thermoelectric modules and the environment, corresponding to two tests, one under forced convection with a wind velocity of 1 m/s (TEST-1) and the other under natural convection conditions (TEST-2). In both tests, a heat flux of 40 W has been applied to the two prototypes, with the thermoelectric modules connected to a load resistance of 2.2 Ω.

It can be observed that the increase in the temperatures produced between the cold face of the module and the environment is greater in the case of the TEG_w/o_RC, which does not incorporate the radiative surface treatment, as a result of a worse heat transfer by radiation. This effect, which becomes more significant in the case of natural convection, determines that the thermal resistance of the HP in this TEG_w/o_RC is higher (see Fig. 6) and the electric power output of the generator is lower, due to the decrease in the temperature difference between the module's faces (see Fig. 7). These tests have been repeated varying the load resistance as well as the heat flux from the hot source, to find the thermal resistance values of the heat exchangers and the electric generation, as described in the methodology.

Fig. 6 shows the results of the thermal resistance of the HPs, comparing the tests in forced and free convection for each of the two prototypes: TEG_RC and TEG_w/o_RC. If the results of the tests in forced convection (TEST-1) are compared, in the same conditions as in the initial TEST-0, it is observed that the TEG_w/o_RC maintains the value of its resistance, 1.72 K/W. However, the TEG_RC, that includes the radiative coating, offers a lower thermal resistance of 1.6 K/W, showing that the surface treatment improves a 7.5 % the thermal resistance value of the heat-pipes.

The greatest change occurs when testing the devices under natural convection conditions (TEST-2), where the radiative treatment was expected to have a higher effect, due to the decrease in the convection coefficient and, therefore, to the greater influence of radiation. In the case of the TEG_w/o_RC, the thermal resistance increases an 86.4 % compared with the case of wind velocity of 1 m/s, reaching an average value of 3.2 K/W. However, in the case of the TEG_RC, the thermal resistance of the heat exchanger corresponds to 54.7 %, reaching on average 2.48 K/W. This represents a 29 % improvement in the thermal resistance of the HPs that include the radiative treatment. In this case, the improvement in the radiation heat transfer makes up for the decrease in the free convection coefficient when there is no air velocity.

The next analysis carried out is about the electric generation of the thermoelectric prototypes. As described in Eq. (5), the electric power output depends on the load resistance to which the TEG is connected, so the performance of each prototype has been tested varying the electric load resistance to obtain the characteristic curve of these devices. Fig. 7 shows the results obtained from the experimentation under forced and

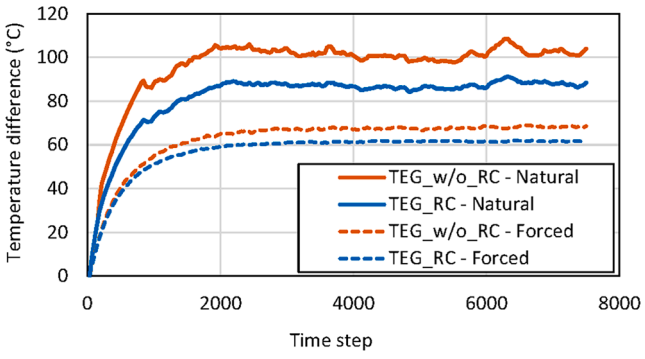

Fig. 5. Evolution of the temperature difference between the cold face of the modules and the environment of both prototypes (TEG_RC and TEG_w/o_RC), for 40 W of heat provided and 2.2 Ω of load resistance.

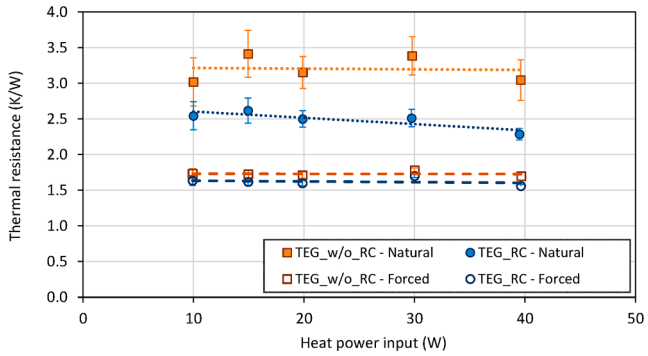

Fig. 6. Results of the thermal resistance of the heat-pipes for the TEG_RC and TEG_w/o_RC, both under forced convection with an air velocity of 1 m/s (TEST-1) and under natural convection (TEST-2), for different heat power inputs.

natural convection, and it is observed that the trend is the expected one for a thermoelectric generator: an initial increase in the electric generation as the load resistance increases up to the optimum point, followed by a decrease in the power output. Comparing the behavior of both prototypes under forced and free conditions, it can be seen that there is hardly any difference in the electric production for low heat fluxes, lower than 20 W. However, with higher heat fluxes, the differences become significant. Under forced convection, TEG_w/o_RC generates 0.48 W, while the TEG_RC reaches a production of 0.52 W, which represents an increase of 8.3 % of the electric power output. Once the forced component of the convection is eliminated and a free convection is established, there is a decrease in the power generation from both prototypes, since, as seen in Fig. 6, the resistance of the heat exchangers on the cold side worsens and, therefore, the generation decreases, as described in Eq. (5), (6) and (8). However, it is remarkable that, while the TEG_w/o_RC reduces its electric generation by 35 %, down to 0.31 W, in the absence of air velocity; the TEG_RC only reduces the electric production by 7.7 %, generating 0.48 W. These results show that the application of the radiative surface treatment to the HPs avoids the drastic decrease in the generated electric power that usually occurs in thermoelectric generators when they work under free convection, keeping the production of electrical energy much more constant.

Additional information of TEST-1 and TEST-2 as the hot and cold temperatures of the thermoelectric modules, environment temperature, electric power output and cold-side thermal resistance of the heat exchangers; is included in Table 3.

Fig. 8 shows the electric power generation for different heat fluxes supplied to the prototypes that are connected to the optimal load resistance. It can be seen that, at low heat fluxes, the differences in generation are really small, but from 20 W of thermal power on, there are noticeable differences between the electric power output under natural and forced convection depending on whether the device has the radiative treatment or not. Thus, for example, for 30 W of heat input under forced convection, TEG_RC is generating 11 % more electric power than the TEG_w/o_RC thanks to the radiative coating. In the case of natural convection, this improvement rises to 38.8 %. When 40 W are applied to the generators this effect becomes more visible, reaching an increase in the electric generation of 54.8 % thanks to the treatment. It is noteworthy that even under natural convection, the electric power output of the TEG_RC is very similar to the electric generation of the TEG_w/o_RC under forced convection. This effect means that the electric production of the thermoelectric generators can be maintained at its best values even in more unfavorable conditions, such as the absence of external air velocity. This improvement can have a large impact on thermoelectric applications such as those developed in [20–22], avoiding energy losses in conditions of no wind.

3.3. Results of outdoor experiments: TEST-3

In this section, the results obtained in the outdoor tests are shown. In these experiments both the ambient temperature and the wind velocity have been recorded since these are conditions that cannot be controlled as they depend on the weather.

Fig. 9 shows the temporal evolution of the temperature difference between the cold face of the thermoelectric modules and the environment temperature, as well as the wind velocity during the test. As it can be seen, there is a clear relationship between that temperature difference achieved and the presence of gusts of wind. With higher wind velocities, where heat transfer mainly occurs by means of forced convection, a temperature difference of around 50 °C is achieved, while, with very low wind velocities, the temperature difference increase, meaning that the heat dissipation is poorer and consequently the thermal resistance of the HPs increases. However, as it has been seen in the tests inside, this rise in the thermal resistance is smaller in the TEG_RC, reaching a temperature difference of 80 °C. Whereas in the TEG_w/o_RC the temperature difference rises up to more than 100 °C.

For both prototypes, these results show that the thermal resistance of the HPs of has a direct influence on the electric generation. As shown in Fig. 10, electric power output rises with an increase in the wind velocity, reaching an average generation of 0.57 W with TEG_RC and 0.56 W with TEG_w/o_RC. This electric generation decreases when the wind slows

Table 3
Experimental values for TEST-1 and TEST-2 under optimal electric load resistance and heat flux of 40 W.

Test	Device	T_H(°C)	T_C(°C)	T_∞(°C)	$\dot{W}_e$(W)	R_C(K/W)
1 (forced)	TEG_RC	130.6	76.2	15.3	0.52	1.60
	TEG_w/o_RC	133.1	82.3	15.3	0.48	1.72
2 (natural)	TEG_RC	151.9	103.2	14.8	0.48	2.29
	TEG_w/o_RC	171.8	126.0	14.8	0.31	3.04

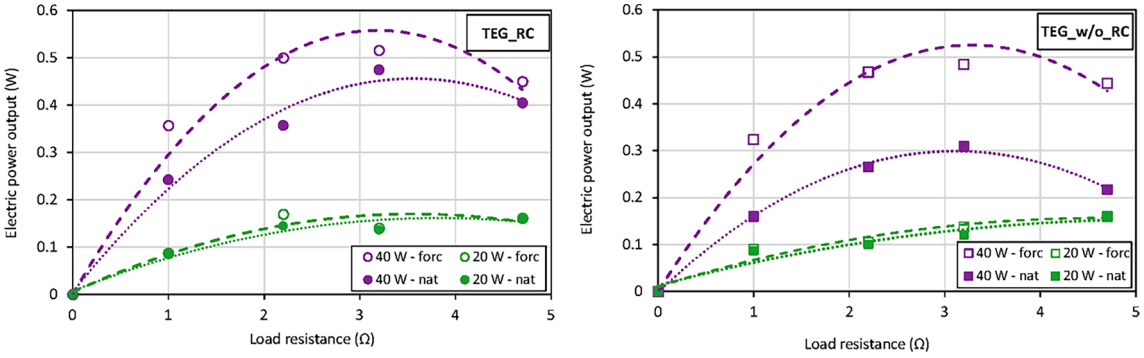

Fig. 7. Electric power output of both TEG prototypes under forced convection, with a wind velocity of 1 m/s (TEST-1) and natural convection (TEST-2), for different load resistances and two heat fluxes provided (20 and 40 W).

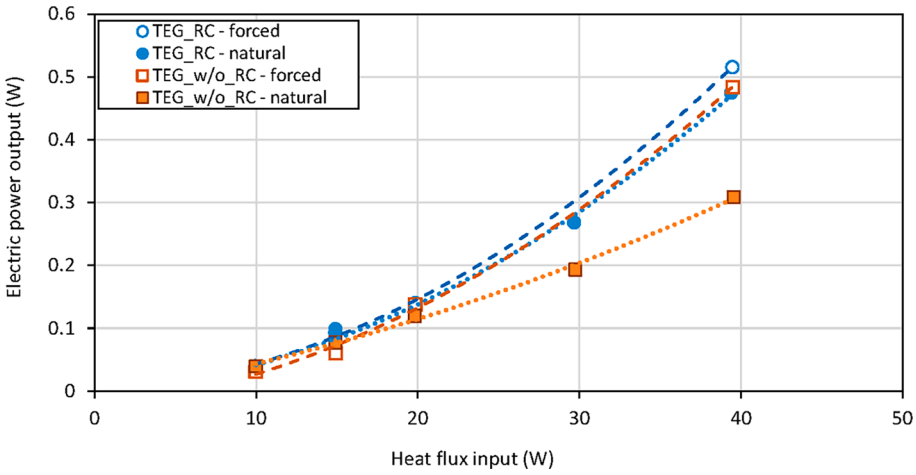

Fig. 8. Electric power output from both TEG prototypes with the optimal load resistance, under natural and free convection (with an air velocity of 1 m/s), varying the heat flux provided.

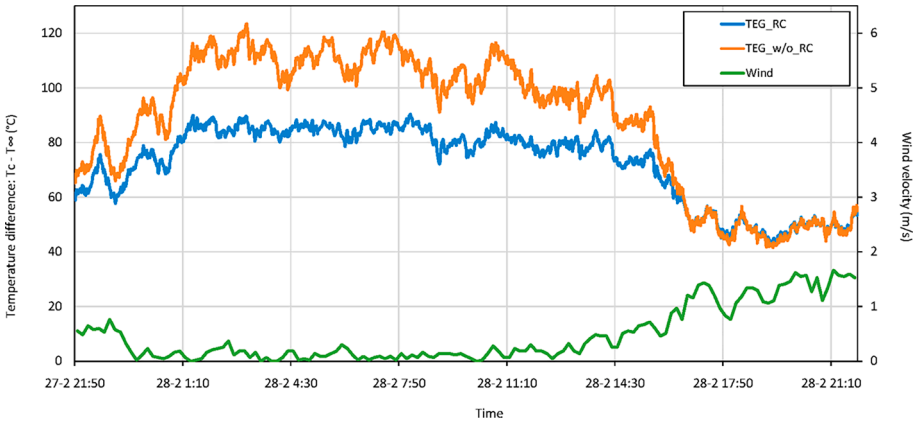

Fig. 9. Evolution of the temperature difference between the cold face of the thermoelectric modules in the generators and the environment temperature; and wind velocity over time during TEST-3.

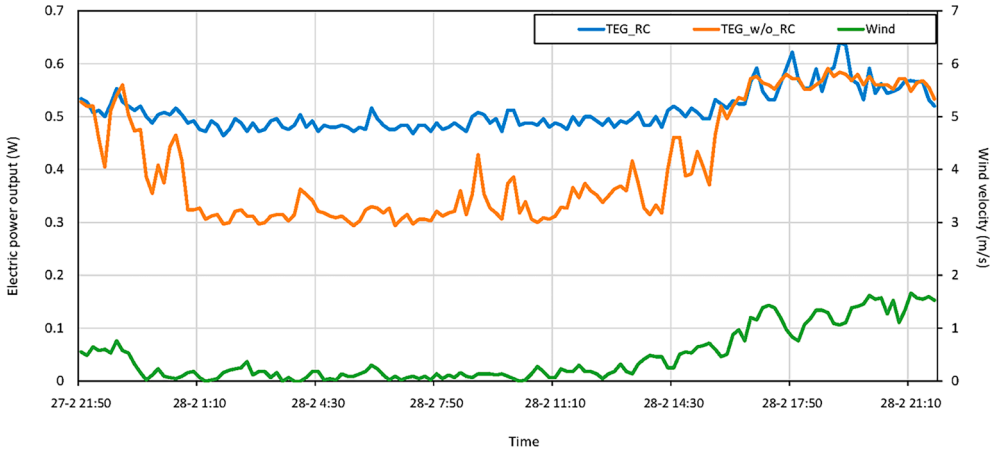

Fig. 10. Electric power output from both prototypes and wind velocity at the test site.

down showing a similar behavior detected in the tests inside the laboratory. During periods with low wind velocities, in which the forced convection component disappears, the electric generation from TEG_RC drops to 0.49 W, which represents a 14 % decrease. While in the case of the TEG_w/o_RC, the generation falls to 0.33 W, a 41.6 % reduction. Again, it is observed that the radiative treatment considerably counteracts the reduction in the electric production caused by a poorer convective heat transfer.

Finally, Table 4 compares the electric generation achieved with both prototypes in all the conditions studied, highlighting the increase in the production of electric power as a result of the radiative treatment placed on the TEG_RC prototype. It is observed that, in all situations, the

Table 4
Comparison of electric power output under all studied conditions, for a heat flux of 40 W.

	Indoors		Outdoors	
	Forced convection (1 m/s)	Natural convection	Forced convection (1.5 m/s)	No wind
TEG_RC	0.52 W	0.48 W	0.57 W	0.49 W
TEG_w/o_RC	0.48 W	0.31 W	0.56 W	0.33 W
Improvement with RC	8.3 %	54.8 %	1.8 %	48.5 %

TEG_RC generates more electricity than the TEG_w/o_RC. This increase in generation is much more noticeable when natural convection condition is dominant (as shown during the indoor tests under free convection or outdoors without wind). Whereas in those cases where forced convection is important, the improvements achieved are reduced.

In the cases of indoor tests, the air velocity recorded in the tests carried out inside the climatic chamber was 1 m/s, while in the case of outdoor wind tests, the speed was 1.5 m/s, which explains why the percentage of improvement due to the radiative treatment is lower, noting the fact that for high wind velocities, forced convection has a dominant effect over radiation.

Table 5 gathers the values of the efficiency achieved by the thermoelectric generators under all the studied conditions. To estimate the conversion efficiency of the generators the electric power output is being divided by the rate of heat flow absorbed from the hot source, according to Equation (13).

$$\eta = \frac{\dot{W}_e}{\dot{Q}_H} \tag{13}$$

As it can be seen, the radiative coating improves again the performance of the device specially under natural or free convection conditions. The maximum efficiency obtained from the experiments gets a value of 1.4 %.

4. Conclusions

For the first time, a radiative surface treatment has been applied to the heat-pipe heat exchanger of a thermoelectric generator to improve the electric power output of the device. In the results of the tests carried out under forced convection conditions, with an air velocity of 1 m/s, the heat-pipes with the coating improved by 7 % the thermal resistance with respect to the heat exchanger without the radiative film. In the case of the tests under natural convection, the thermal resistances of both devices increased. However, while in the case of the TEG without the radiative treatment, the thermal resistance increased by 86.4 %, the thermal resistance of the TEG with the treatment only increased by 54.7 %, which means that the heat-pipes with the radiative coating offer a 29 % less thermal resistance.

This improvement in the heat exchangers is reflected in the electric power output that both prototypes are capable of generating. Under forced convection a maximum electric production of 0.52 W is achieved with the TEG with the radiative cooling treatment, and 0.48 W with the TEG without the coating. As it could be expected, under natural convection conditions, the electric generation decreases. However, this generation drop is only of 7.7 % with the TEG_RC, while with the TEG_w/o_RC the decrease is 35.4 %, proving that the radiative film greatly minimizes the loss of electric generation that occurs in the absence of forced convection with the heat-pipes.

The experimental tests performed outdoors, with changing weather conditions, are in agreement with those carried out in the laboratory, showing that when the wind velocity is very low or null, the temperature difference between the cold face of the thermoelectric modules and the environment increases, although to a lesser extent in the TEG that includes de radiative coating. This effect has a positive influence on the electric generation, which, although it decreases when there is no wind, the reduction is only of 14 % thanks to the radiative surface treatment. Meanwhile, in the TEG without the radiative coating, the generation falls by 41.6 %.

Table 5
Comparison of the conversion efficiency of the generators under all studied conditions, for a heat flux of 40 W.

	Indoors		Outdoors	
	Forced convection (1 m/s)	Natural convection	Forced convection (1.5 m/s)	No wind
TEG_RC	1.28 %	1.19 %	1.40 %	1.38 %
TEG_w/o_RC	1.19 %	0.77 %	1.21 %	0.82 %
Improvement with RC	8.2 %	54.2 %	16.1 %	68.73 %

In short, it has been proven that the radiative coating over the heat-pipes of the cold side heat exchangers has a positive influence on the heat dissipation from the thermoelectric modules to the environment. This translated into an increase in the electric production of the thermoelectric generator of 8.3 % with outdoor wind velocities of 1 m/s and up to 54.8 % when the device is working under free convection conditions. This increase in the electric generation of thermoelectric devices is very interesting, since it is an improvement in the heat exchangers that does not imply the incorporation of moving parts, nor loss of robustness or compactness, typical of thermoelectric systems.

CRediT authorship contribution statement

David Astrain: Conceptualization, Methodology, Validation, Investigation, Writing – original draft, Supervision. **Juliana Jaramillo-Fernandez:** Methodology, Validation, Investigation, Writing – original draft, Writing – review & editing, Supervision. **Miguel Araiz:** Methodology, Investigation, Data curation, Writing – original draft, Writing – review & editing. **Achille Francone:** Methodology, Investigation. **Leyre Catalán:** Methodology, Investigation, Data curation, Writing – review & editing. **Alejandra Jacobo-Martín:** Methodology, Investigation, Writing – review & editing. **Patricia Alegría:** Methodology, Investigation, Writing – review & editing. **Clivia M. Sotomayor-Torres:** Writing – review & editing, Supervision.

Declaration of Competing Interest

The authors declare that they have no known competing financial interests or personal relationships that could have appeared to influence the work reported in this paper.

Data availability

No data was used for the research described in the article.

Acknowledgements

The authors acknowledge the support of the Spanish Ministry of Science, Innovation and Universities, and the European Regional Development Fund, under grants PID2021-124014OB-I00 (VIVOTEG), TED2021-129359B-I00 (GEOTEG), PGC2018-101743-B-I00 (SIP) and RTI2018-093921-A-C44 (SMOOTH). The ICN2 authors thank the CERCA Program/Generalitat de Catalunya. **Open access funding provided by Universidad Pública de Navarra**.

Appendix A. Supplementary material

Supplementary data to this article can be found online at https://doi.org/10.1016/j.applthermaleng.2023.120162.

References

[1] S.M. Pourkiaei, M.H. Ahmadi, M. Sadeghzadeh, S. Moosavi, F. Pourfayaz, L. Chen, M.A. Pour Yazdi, R. Kumar, Thermoelectric cooler and thermoelectric generator devices: a review of present and potential applications, modeling and materials, Energy 186 (2019), 115849, https://doi.org/10.1016/j.energy.2019.07.179.

[2] D. Champier, Thermoelectric generators: A review of applications, Energy Convers Manag. 140 (2017) 167–181, https://doi.org/10.1016/j.enconman.2017.02.070.

[3] W. He, G. Zhang, X. Zhang, J. Ji, G. Li, X. Zhao, Recent development and application of thermoelectric generator and cooler, Appl. Energy 143 (2015), https://doi.org/10.1016/j.apenergy.2014.12.075.

[4] A. Montecucco, J. Siviter, A.R. Knox, A Combined Heat and Power System for Solid-fuel Stoves Using Thermoelectric Generators, Energy Procedia 75 (2015) 597–602, https://doi.org/10.1016/j.egypro.2015.07.462.

[5] X.F. Zheng, C.X. Liu, R. Boukhanouf, Y.Y. Yan, W.Z. Li, Experimental study of a domestic thermoelectric cogeneration system, Appl. Therm. Eng. 62 (2014) 69–79, https://doi.org/10.1016/j.applthermaleng.2013.09.008.

[6] A. Mohammadnia, A. Rezania, B.M. Ziapour, F. Sedaghati, L. Rosendahl, Hybrid energy harvesting system to maximize power generation from solar energy, Energy Convers Manag. 205 (2020), 112352, https://doi.org/10.1016/j.enconman.2019.112352.

[7] M.A. Karri, E.F. Thacher, B.T. Helenbrook, Exhaust energy conversion by thermoelectric generator: Two case studies, Energy Convers Manag. 52 (2011) 1596–1611, https://doi.org/10.1016/j.enconman.2010.10.013.

[8] F. Huang, J. Zheng, J.M. Baleynaud, J. Lu, Heat recovery potentials and technologies in industrial zones, J. Energy Inst. 90 (2017) 951–961, https://doi.org/10.1016/j.joei.2016.07.012.

[9] D. Zhao, G. Tan, A review of thermoelectric cooling: Materials, modeling and applications, Appl. Therm. Eng. 66 (2014) 15–24, https://doi.org/10.1016/j.applthermaleng.2014.01.074.

[10] D. Astrain, J.G. Vián, A. Martínez, A. Rodríguez, Study of the influence of heat exchangers' thermal resistances on a thermoelectric generation system, Energy 35 (2010) 602–610, https://doi.org/10.1016/j.energy.2009.10.031.

[11] X. Niu, J. Yu, S. Wang, Experimental study on low-temperature waste heat thermoelectric generator, J. Power Sources 188 (2009) 621–626, https://doi.org/10.1016/j.jpowsour.2008.12.067.

[12] T.Y. Kim, A.A. Negash, G. Cho, Waste heat recovery of a diesel engine using a thermoelectric generator equipped with customized thermoelectric modules, Energy Convers Manag. 124 (2016) 280–286, https://doi.org/10.1016/j.enconman.2016.07.013.

[13] P. Aranguren, D. Astrain, M.G. Pérez, Computational and experimental study of a complete heat dissipation system using water as heat carrier placed on a thermoelectric generator, Energy 74 (2014) 346–358, https://doi.org/10.1016/j.energy.2014.06.094.

[14] Y. Liu, Z. Shi, G. Wang, Y. Yan, Y. Zhang, Experimental Investigation for a Novel Prototype of a Thermoelectric Power Generator With Heat Pipes, Front. Energy Res. 9 (2021) 1–13, https://doi.org/10.3389/fenrg.2021.744366.

[15] P. Aranguren, D. Astrain, A. Rodríguez, A. Martínez, Experimental investigation of the applicability of a thermoelectric generator to recover waste heat from a combustion chamber, Appl. Energy 152 (2015) 121–130, https://doi.org/10.1016/j.apenergy.2015.04.077.

[16] A. Date, A. Date, C. Dixon, R. Singh, A. Akbarzadeh, Theoretical and experimental estimation of limiting input heat flux for thermoelectric power generators with passive cooling, Sol. Energy 111 (2015) 201–217, https://doi.org/10.1016/j.solener.2014.10.043.

[17] B. Orr, B. Singh, L. Tan, A. Akbarzadeh, Electricity generation from an exhaust heat recovery system utilising thermoelectric cells and heat pipes, Appl. Therm. Eng. 73 (2014) 586–595, https://doi.org/10.1016/j.applthermaleng.2014.07.056.

[18] M. Araiz, A. Martínez, D. Astrain, P. Aranguren, Experimental and computational study on thermoelectric generators using thermosyphons with phase change as heat exchangers, Energy Convers Manag. 137 (2017) 155–164, https://doi.org/10.1016/j.enconman.2017.01.046.

[19] Y. Huang, D. Xu, J. Kan, W. Li, Study on field experiments of forest soil thermoelectric power generation devices, PLoS One 14 (2019) 1–13, https://doi.org/10.1371/journal.pone.0221019.

[20] L. Catalan, M. Araiz, P. Aranguren, G.D. Padilla, P.A. Hernandez, N.M. Perez, C. G. de la Noceda, J.F. Albert, D. Astrain, Prospects of autonomous volcanic monitoring stations: Experimental investigation on thermoelectric generation from fumaroles, Sensors (Switzerland). 20 (2020) 1–21, https://doi.org/10.3390/s20123547.

[21] L. Catalan, A. Garacochea, A. Casi, M. Araiz, P. Aranguren, D. Astrain, Experimental evidence of the viability of thermoelectric generators to power volcanic monitoring stations, Sensors (Switzerland). 20 (2020) 1–25, https://doi.org/10.3390/s20174839.

[22] P. Alegria, L. Catalan, M. Araiz, A. Rodriguez, D. Astrain, Experimental development of a novel thermoelectric generator without moving parts to harness shallow hot dry rock fields, Appl. Therm. Eng. 200 (2022), 117619, https://doi.org/10.1016/j.applthermaleng.2021.117619.

[23] W.M. Rohsenow, Handbook of Heat Transfer, 1998.

[24] A.P. Raman, M.A. Anoma, L. Zhu, E. Rephaeli, S. Fan, Passive radiative cooling below ambient air temperature under direct sunlight, Nature 515 (2014) 540–544.

[25] Y. Zhu, D. Wang, C. Fang, P. He, Y.H. Ye, A multilayer emitter close to ideal solar reflectance for efficient daytime radiative cooling, Polymers (Basel). 11 (2019) 1–10, https://doi.org/10.3390/polym11071203.

[26] A. Hervé, J. Drévillon, Y. Ezzahri, K. Joulain, Radiative cooling by tailoring surfaces with microstructures: Association of a grating and a multi-layer structure, J. Quant. Spectrosc. Radiat. Transf. 221 (2018) 155–163, https://doi.org/10.1016/j.jqsrt.2018.09.015.

[27] S. Meng, L. Long, Z. Wu, N. Denisuk, Y. Yang, L. Wang, F. Cao, Y. Zhu, Scalable dual-layer film with broadband infrared emission for sub-ambient daytime radiative cooling, Sol. Energy Mater. Sol. Cells 208 (2020), 110393, https://doi.org/10.1016/j.solmat.2020.110393.

[28] E. Blandre, R.A. Yalçin, K. Joulain, J. Drévillon, Microstructured surfaces for colored and non-colored sky radiative cooling, Opt. Express 28 (2020) 29703–29713, https://doi.org/10.1364/OE.401368.

[29] J. Jaramillo-Fernandez, G.L. Whitworth, J.A. Pariente, A. Blanco, P.D. Garcia, C. Lopez, C.M. Sotomayor-Torres, A Self-Assembled 2D Thermofunctional Material for Radiative Cooling, Small 15 (2019) 1905290, https://doi.org/10.1002/smll.201905290.

[30] G.L. Whitworth, J. Jaramillo-Fernandez, J.A. Pariente, P.D. Garcia, A. Blanco, C. Lopez, C.M. Sotomayor-Torres, Simulations of micro-sphere/shell 2D silica photonic crystals for radiative cooling, Opt. Express 29 (2021) 16857–16866, https://doi.org/10.1364/OE.420989.

[31] S. Atiganyanun, J.B. Plumley, S.J. Han, K. Hsu, J. Cytrynbaum, T.L. Peng, S. M. Han, S.E. Han, Effective Radiative Cooling by Paint-Format Microsphere-Based Photonic Random Media, ACS Photonics 5 (2018) 1181–1187, https://doi.org/10.1021/acsphotonics.7b01492.

[32] E. Rephaeli, A. Raman, S. Fan, Ultrabroadband Photonic Structures To Achieve High-Performance Daytime Radiative Cooling, Nano Lett. 13 (2013) 1457–1461, https://doi.org/10.1021/nl4004283.

[33] Z. Huang, X. Ruan, Nanoparticle embedded double-layer coating for daytime radiative cooling, Int. J. Heat Mass Transf. 104 (2017) 890–896, https://doi.org/10.1016/j.ijheatmasstransfer.2016.08.009.

[34] C. Yijun, M. Jyotirmoy, L. Wenxi, S.-W. Ajani, T. Cheng-Chia, H. Wenlong, S. Sajan, Y. Nanfang, H.R.P. S., C. Anyuan, Y. Yuan, Colored and paintable bilayer coatings with high solar-infrared reflectance for efficient cooling, Sci Adv. 6 (2021) eaaz5413. https://doi.org/10.1126/sciadv.aaz5413.

[35] A. Leroy, B. Bhatia, C.C. Kelsall, A. Castillejo-Cuberos, M. di Capua H., L. Zhao, L. Zhang, A.M. Guzman, E.N. Wang, High-performance subambient radiative cooling enabled by optically selective and thermally insulating polyethylene aerogel, Sci Adv. 5 (2019) eaat9480. https://doi.org/10.1126/sciadv.aat9480.

[36] M. Yang, W. Zou, J. Guo, Z. Qian, H. Luo, S. Yang, N. Zhao, L. Pattelli, J. Xu, D. S. Wiersma, Bioinspired "Skin" with Cooperative Thermo-Optical Effect for Daytime Radiative Cooling, ACS Appl. Mater. Interfaces 12 (2020) 25286–25293, https://doi.org/10.1021/acsami.0c03897.

[37] H. Zhang, K.C.S. Ly, X. Liu, Z. Chen, M. Yan, Z. Wu, X. Wang, Y. Zheng, H. Zhou, T. Fan, Biologically inspired flexible photonic films for efficient passive radiative cooling, PNAS 117 (2020) 14657–14666, https://doi.org/10.1073/pnas.2001802117.

[38] D. Li, X. Liu, W. Li, Z. Lin, B. Zhu, Z. Li, J. Li, B. Li, S. Fan, J. Xie, J. Zhu, Scalable and hierarchically designed polymer film as a selective thermal emitter for high-performance all-day radiative cooling, Nat. Nanotechnol. 16 (2021) 153–158, https://doi.org/10.1038/s41565-020-00800-4.

[39] X. Wang, X. Liu, Z. Li, H. Zhang, Z. Yang, H. Zhou, T. Fan, Scalable Flexible Hybrid Membranes with Photonic Structures for Daytime Radiative Cooling, Adv. Funct. Mater. 30 (2020) 1907562, https://doi.org/10.1002/adfm.201907562.

[40] W. Huang, Y. Chen, Y. Luo, J. Mandal, W. Li, M. Chen, C.-C. Tsai, Z. Shan, N. Yu, Y. Yang, Scalable Aqueous Processing-Based Passive Daytime Radiative Cooling Coatings, Adv. Funct. Mater. 31 (2021) 2010334, https://doi.org/10.1002/adfm.202010334.

[41] J. Mandal, Y. Fu, A.C. Overvig, M. Jia, K. Sun, N.N. Shi, H. Zhou, X. Xiao, N. Yu, Y. Yang, Hierarchically porous polymer coatings for highly efficient passive daytime radiative cooling, Science 362 (2018) (1979) 315–319.

[42] M. Yang, M. Yang, W. Zou, W. Zou, J. Guo, J. Guo, Z. Qian, Z. Qian, H. Luo, H. Luo, S. Yang, S. Yang, N. Zhao, N. Zhao, L. Pattelli, L. Pattelli, J. Xu, D.S. Wiersma, D. S. Wiersma, Bioinspired "skin" with Cooperative Thermo-Optical Effect for Daytime Radiative Cooling, ACS Appl. Mater. Interfaces 12 (2020) 25286–25293, https://doi.org/10.1021/acsami.0c03897.

[43] S. Gamage, D. Banerjee, M.M. Alam, T. Hallberg, C. Åkerlind, A. Sultana, R. Shanker, M. Berggren, X. Crispin, H. Kariis, D. Zhao, M.P. Jonsson, Reflective and transparent cellulose-based passive radiative coolers, Cellul. (2021), https://doi.org/10.1007/s10570-021-04112-1.

[44] B. Xiang, R. Zhang, Y. Luo, S. Zhang, L. Xu, H. Min, S. Tang, X. Meng, 3D porous polymer film with designed pore architecture and auto-deposited SiO2 for highly efficient passive radiative cooling, Nano Energy 81 (2021), 105600, https://doi.org/10.1016/j.nanoen.2020.105600.

[45] X. Chen, M. He, S. Feng, Z. Xu, H. Peng, S. Shi, C. Liu, Y. Zhou, Cellulose-based porous polymer film with auto-deposited TiO2 as spectrally selective materials for passive daytime radiative cooling, Opt Mater (Amst). 120 (2021), 111431, https://doi.org/10.1016/j.optmat.2021.111431.

[46] Y. Chen, B. Dang, J. Fu, C. Wang, C. Li, Q. Sun, H. Li, Cellulose-Based Hybrid Structural Material for Radiative Cooling, Nano Lett. 21 (2021) 397–404, https://doi.org/10.1021/acs.nanolett.0c03738.

[47] S. Gamage, E.S.H. Kang, C. Åkerlind, S. Sardar, J. Edberg, H. Kariis, T. Ederth, M. Berggren, M.P. Jonsson, Transparent nanocellulose metamaterial enables

controlled optical diffusion and radiative cooling, J Mater Chem C Mater. 8 (2020) 11687–11694, https://doi.org/10.1039/D0TC01226B.
[48] W. Wei, Y. Zhu, Q. Li, Z. Cheng, Y. Yao, Q. Zhao, P. Zhang, X. Liu, Z. Chen, F. Xu, Y. Gao, An Al2O3-cellulose acetate-coated textile for human body cooling, Sol. Energy Mater. Sol. Cells 211 (2020), 110525, https://doi.org/10.1016/j.solmat.2020.110525.
[49] J. Jaramillo-Fernandez, H. Yang, L. Schertel, G.L. Whitworth, P.D. Garcia, S. Vignolini, C.M. Sotomayor-Torres, Highly-scattering cellulose-based lms for radiative cooling, Adv. Sci. 2104758 (2021), https://doi.org/10.1002/advs.202104758.
[50] Z. Zhan, M. ElKabbash, Z. Li, X. Li, J. Zhang, J. Rutledge, S. Singh, C. Guo, Enhancing thermoelectric output power via radiative cooling with nanoporous alumina, Nano Energy 65 (2019), 104060, https://doi.org/10.1016/j.nanoen.2019.104060.
[51] D.M. Rowe, Thermoelectrics Handbook: Macro to Nano, 1st ed., Boca Raton, 2006.
[52] Marlow Industries Inc., Marlow TG12-8 Datasheet, (2016) 1–2. http://www.marlow.com/media/marlow/product/downloads/tg12-8-01ls/TG12-8_Data_Sheet_RevM.pdf (accessed January 1, 2016).
[53] R.P. S.A.U., ProRox WM 970 Datasheet, 2012.
[54] Armacell, ArmaFlex insulation Datasheet, 2021.
[55] M.A. Verschuuren, M. Megens, Y. Ni, H. van Sprang, A. Polman, Large area nanoimprint by substrate conformal imprint lithography (SCIL), Adv. Opt. Technol. 6 (2017) 243–264, https://doi.org/10.1515/aot-2017-0022.
[56] B. Kwon, J.H. Kim, Importance of Molds for Nanoimprint Lithography: Hard, Soft, and Hybrid Molds, J. Nanosci. 2016 (2016) 6571297, https://doi.org/10.1155/2016/6571297.
[57] I. Rodríguez, J. Hernández, Soft thermal nanoimprint and hybrid processes to produce complex structures, Nanofabrication: Nanolithography Techniques and Their Applications. 7 (2020) 1–33.
[58] N. Kehagias, A. Francone, M. Guttmann, F. Winkler, A. Fernández, C.M. Sotomayor Torres, Fabrication and replication of re-entrant structures by nanoimprint lithography methods, J. Vac. Sci. Technol. B 36 (2018) 06JF01, https://doi.org/10.1116/1.5048241.
[59] S.WG. Coleman HW, Experimentation, validation and uncertainty analysis for engineers., n.d. https://doi.org/https://doi.org/10.1017/CBO9781107415324.004.